R. Vescovini, V. Oliveri, D. Pizzi, L. Dozio, P.M. Weaver
Pre-Buckling and Buckling Analysis of Variable-Stiffness, Curvilinearly Stiffened Panels
Aerotecnica, Missili e Spazio, In press - Published online 10/12/2019
doi:10.1007/s42496-019-00031-4

Aerotecnica Missili & Spazio manuscript No.
(will be inserted by the editor)

Pre-Buckling and Buckling Analysis of Variable-Stiffness, Curvilinearly Stiffened Panels

R. Vescovini · V. Oliveri · D. Pizzi · L. Dozio · P.M. Weaver

Received: date / Accepted: date

Abstract This work illustrates a fast numerical approach for analyzing the pre-buckling and buckling response of innovative panel configurations for aerospace structures. Specifically, the approach allows composite panels with variable-stiffness skins and stiffened by curvilinear stringers to be studied in a fast yet accurate manner. The method of Ritz is applied in conjunction with first-order theories for modeling the skin and the stiffeners, the former described referring to Mindlin plate theory, the latter to Timoshenko beam model. Due to the excellent convergence properties of the approach, pre-buckling stress distributions can be captured with reduced effort. Similarly, accurate buckling predictions can be obtained with relatively few degrees of freedom, much less with respect to typical models relying upon the use of finite elements. Results are presented for a number of test-cases from the literature, illustrating the potential of the proposed approach as a mean for performing preliminary studies with reduced computational effort.

Keywords Curvilinear stringers · Variable-stiffness · Stiffened panels · Ritz method

1 Introduction

Aerospace structural panels have been classically designed using orthogonal stiffening elements, i.e. stringers along the longitudinal directions and ribs/frames along the transverse one. However, improved tailoring opportunities are available by exploiting the concept of stiffness variability, using tow-steering and curvilinear stringers, separately or in combination. Potential gains offered by tow-steered panels are well-documented in the literature [1–5], and several studies clearly illustrated the possibility of improving buckling and post-buckling responses with respect to corresponding quasi-isotropic configurations. Recent works addressed also the effects of different kinematic theories when applied to the analysis of tow-steered panels [3,6,7].
In the past years, it was demonstrated that curvilinear stringers can be successfully used to further improve stiffness tailoring opportunities and, to a more general extent, the structural efficiency of stiffened panels. Pioneering work in this field is due to Kapania and co-workers [8,9], who discussed the possibility of reducing static stresses and improving buckling loads, in particular for shear-dominated loading conditions [10].
In the past, ad-hoc finite element strategies were developed to facilitate the analysis of curvilinearly stiffened panels. Indeed, one crucial aspect regards the generation of regular grids, despite the presence of non-straight

R. Vescovini, L. Dozio and D. Pizzi
Dip. Scienze e Tecnologie Aerospaziali, Politecnico di Milano, Italy
E-mail: riccardo.vescovini@polimi.it

V. Oliveri and P.M. Weaver
School of Engineering and Bernal Institute, University of Limerick, Ireland

stiffeners. To this aim, a finite element incorporating the stiffener element, whose displacement field is interpolated starting from the skin, was proposed in Refs. [11–13]
Another effective strategy consists in adopting a mesh-free approach, so that any issue due to the generation of the model is essentially removed. This approach was pursued in Refs. [14–19]. Recently, curvilinearly stiffened panels were analyzed via mesh-free strategies by Yoshida et al. [20] and Ozdemir et al. [21], modeling the stringers as ideal constraints and explicit assemblies of shell elements, respectively. Recently, the concept of variable-stiffness skin in conjunction with curvilinear stringers has been proposed in the context of finite-element procedures [22–24]. Optimization studies were carried out to highlight potential advantages with respect to straight-fiber configurations.
Given the inherent geometrical complexity of variable-stiffness (VS) panels with curvilinear stringers, the development of efficient computational tools plays a crucial role in facilitating preliminary design studies and investigating potential benefits. In this context, semi-analytical procedures have been successfully applied in the past years for analyzing composite structures (see, e.g. [25–30]).

In this paper, illustrated is a simplified procedure for assessing the structural response – emphasis is given here to the pre-buckling and buckling response – of VS curvilinearly stiffened panels. The procedure is fast in so far as relies upon the method of Ritz, where the structure is modelled as an assembly of plate and beam elements. The displacement field is approximated using orthogonal polynomials, guaranteeing convergence of the solution with a relatively small number of degrees of freedom, much smaller with respect to those required by an equivalent Finite Element (FE) analysis. The accuracy of the predictions is shown by comparison against FE simulations and results from the literature, illustrating the potential of the proposed tool as a valuable mean for performing parametric studies and preliminary optimizations.

2 Fast Numerical Approach

The approach is developed in the framework of a displacement-based approach, where the governing equations are derived from a variational formulation of the problem. The approximate solution is retrieved referring to the Ritz method, leading to the solution of discrete problems characterized by a relatively small number of degrees of freedom.
A sketch of the structure under investigation is provided in Figure 1.

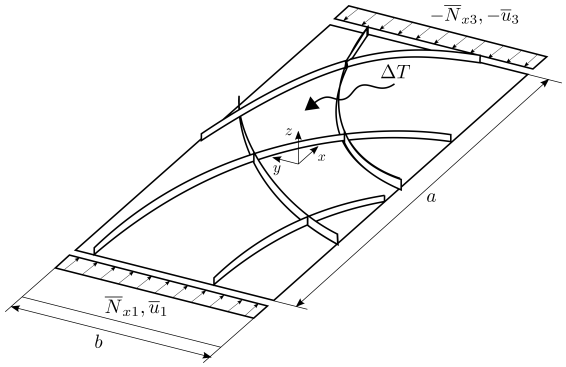

Fig. 1 Sketch of a stiffened panel with three curvilinear stringers – dimensions and conventions for edge loads and prescribed displacements.

A reference system *xyz* is defined at the center of the panel, whose longitudinal and transverse dimensions are denoted as a and b, respectively. Any boundary condition can be accounted for, and loading conditions are defined in the form of prescribed displacements and forces. Note, the sketch illustrates compressive loading conditions, but any other set of loads can be considered within the proposed analysis framework.

2.1 Plate model

The plate model refers to well-known first-order shear deformation theory (FSDT) [31]. One advantage offered by this model – in addition to the possibility of accounting for transverse shear deformability effects – consists in the ease in enforcing continuity of rotations between skin and stiffeners. According to FSDT, the displacement field is expressed as:

$$\begin{aligned} u(x,y,z) &= u_0(x,y) + zL\varphi(x,y) \\ &= [I \quad zL] \begin{Bmatrix} u_0 \\ \varphi \end{Bmatrix} = [I \quad zL]\, d_0 \end{aligned} \tag{1}$$

where the vectors u_0, φ collect the generalized displacement components, i.e. $u_0 = \{u_0 \quad v_0 \quad w_0\}^{\mathrm{T}}$ and $\varphi = \{\varphi_x \quad \varphi_y \quad \varphi_z\}^{\mathrm{T}}$. The matrix L has dimension 3×3, the only not-null contributions being the unitary values at the positions $(1,1)$ and $(2,2)$.
By differentiating the displacement components it is possible to retrieve the strains as function of the kinematic model strain parameters, which are collected into the vector e as:

$$e = \left\{ \xi^{\mathrm{T}} \quad k^{\mathrm{T}} \quad \gamma^{\mathrm{T}} \right\}^{\mathrm{T}} \tag{2}$$

The entries of Eq. (2) represent the membrane, curvature and transverse-shear deformation parameters, respectively.
The skin of the panel is characterized by variable in-plane properties, with fiber orientation defined using Lagrange interpolation in an arbitrary number of points as:

$$\theta(x,y) = \sum_{m=0}^{M-1} \sum_{n=0}^{N-1} \theta_{mn} \prod_{m \neq i} \left(\frac{|x| - x_i}{x_m - x_i} \right) \prod_{n \neq j} \left(\frac{|y| - y_j}{y_n - y_j} \right) \tag{3}$$

Linear fiber orientation variation and straight fiber configurations are retrieved as special cases. As illustrated next, the variability of elastic properties does not alter the framework for formulating the plate problem. In this regard, the governing equations are the same of classical straight-fiber configurations. However, non-constant elastic properties have the effect of coupling the in-plane integrals due to the Ritz approximation. Thus special care is needed in the implementation to keep at minimum the computational time.

2.2 Stiffener model

Dealing with curvilinear stringers, the first step consists in defining the geometry in terms of path. To this aim, a Bézier description is used, where the stiffener coordinates are given as:

$$x(q) = \sum_{i=0}^{n} \binom{n}{i} P_i \, (1-q)^{n-i} \, q^i \qquad \text{with } q \in [0 \quad 1] \tag{4}$$

where the vectors P_i specify the coordinates of the control points.
Once the geometric parametrization is available, the tangent vector, at any point, is obtained as:

$$t = x_{,s} \tag{5}$$

where s is the arc-length coordinate. One can observe that the relation between the parameter p and the arc-length differentials is:

$$\mathrm{d}s = ||x_{,p}||\, \mathrm{d}p = J_{\mathrm{s}}\, \mathrm{d}p \tag{6}$$

with J_s representing the Jacobian of the transformation.
The beam kinematic model is based on Timoshenko beam theory. According to this model, the displacement field for the generic stiffener i is:

$$u^i(s,n,b) = u_0^i(s) + (d_\times)^{\mathrm{T}}\,\theta^i(s) \tag{7}$$

having denoted with s,n,b the coordinates in the curvilinear reference system where $n=t$ and b are the normal and binormal vectors, respectively. For ease of derivation, the origin of the system is taken in correspondence of the skin midsurface.
Note that u_0^i and θ^i define the displacements and the rotations around the three axes, while d is the position vector.
Following Refs. [32, 16], the beam strains can be expressed as:

$$\varepsilon^i = \begin{Bmatrix} u^i_{0,s}\cdot t \\ u^i_{0,s}\cdot n - \theta^i\cdot b \\ u^i_{0,s}\cdot b + \theta^i\cdot n \end{Bmatrix} + (d_\times)^{\mathrm{T}} \begin{Bmatrix} \theta^i_{,s}\cdot t \\ \theta^i_{,s}\cdot t \\ \theta^i_{,s}\cdot t \end{Bmatrix} + \eta^i \tag{8}$$

the first and the second expanded vectors representing the axial strains and the curvatures; the last contribution, η^i stems from the linearization of the Green-Lagrange strain tensor and is introduced for the buckling solution procedure only.
The compatibility between stringers and skin is enforced in a strong-form manner by expressing the beam displacement components as function of the plate generalized displacements. This is done by ensuring that:

$$\begin{cases} u_0^i = u_0|_{\Gamma^i} \\ \theta^i = \mathscr{J}^{\mathrm{T}}\varphi|_{\Gamma^i} \end{cases} \tag{9}$$

where the matrix $\mathscr{J}$ is introduced to transform the skin rotation parameters into rotations around the orthogonal axes xyz.

2.3 Pre-buckling

The pre-buckling analysis is conducted by assuming linear behaviour, and referring to the minimum potential energy principle to derive the equilibrium conditions. The total potential energy is the sum of skin and stiffeners contributions, and the relevant variational principle reads:

$$\delta\Pi = \delta\left(U + W_{\mathrm{m}} + W_{\mathrm{th}} + \sum_{i=1}^{\mathrm{N_s}} \Pi^i\right) = 0 \tag{10}$$

where N_s is the number of stringers.
The strain energy U is [31]:

$$U = \frac{1}{2}\int_{\mathrm{A}} \begin{Bmatrix} \xi \\ k \\ \gamma \end{Bmatrix}^{\mathrm{T}} \begin{bmatrix} A & B & 0 \\ B & D & 0 \\ 0 & 0 & A^{\mathrm{s}} \end{bmatrix} \begin{Bmatrix} \xi \\ k \\ \gamma \end{Bmatrix} \mathrm{dA} = \frac{1}{2}\int_{\mathrm{A}} e^{\mathrm{T}} D_{\mathrm{p}} e\,\mathrm{dA} \tag{11}$$

with obvious definition of the vector e and the plate constitutive matrix D_{p}.
It is important to remark that $D_{\mathrm{p}} = D_{\mathrm{p}}(x,y)$ as fiber orientations are, in general, function of the in-plane position (see Eq. (3)).
The contribution due to mechanical loads is restricted to the prescribed forces (as prescribed displacements are part of the essential conditions of the problem) and is:

$$W_{\mathrm{m}} = -\sum_{i=1}^{4}\int_{\partial \mathrm{A_i}} \left(u_0\overline{N}_{xi} + v_0\overline{N}_{yi}\right)\mathrm{d}\partial\mathrm{A}_i \tag{12}$$

where the summatory is taken at the four edges of the plate. In a similar fashion, the energy term due to thermal loads can be obtained as:

$$W_{\text{th}} = -\int_{\text{A}} e^{\text{T}} \hat{R}(x,y)\,\text{dA}\,\Delta T \tag{13}$$

where $\hat{R}$ are the unitary thermal loads, e is defined in Eq. (2), and ΔT is the uniform temperature variation, taken positive for heating.
The stiffener contribution to the total strain energy can be written as:

$$U^i = \frac{1}{2}\int_{\Gamma^i} \begin{Bmatrix} \tilde{\xi}^i \\ \tilde{k}^i \end{Bmatrix}^{\text{T}} \left[C^i \begin{Bmatrix} \tilde{\xi}^i \\ \tilde{k}^i \end{Bmatrix} + \begin{Bmatrix} \hat{F}^i \\ \hat{M}^i \end{Bmatrix} \Delta T \right] \text{d}s \tag{14}$$

having denoted with a tilde the beam strain parameters once compatibility with the skin dislacements is enforced, and with C^i the section constitutive matrix [33].

2.4 Buckling

Buckling equations are derived referring to the Trefftz's criterion. By splitting the contributions due to the skin and stiffeners, the reading variational principle is:

$$\delta\left(\delta^2\Pi + \sum_{i=1}^{\text{N}_\text{s}} \delta^2\Pi^i\right) = 0 \tag{15}$$

The first entry accounts for the quadratic part of the skin strain energy, which is:

$$\delta^2\Pi = \frac{1}{2}\int_{\text{A}} e^{\text{T}} D_{\text{p}} e\,\text{dA} + \frac{1}{2}\int_{\text{A}} \left[\text{N}_{\text{xx}}^{\text{pre}}(\text{x},\text{y})\text{w}_{0,\text{x}}^2 + 2\text{N}_{\text{xy}}^{\text{pre}}(\text{x},\text{y})\text{w}_{0,\text{x}}\text{w}_{0,\text{y}} + \text{N}_{\text{yy}}^{\text{pre}}(\text{x},\text{y})\text{w}_{0,\text{y}}^2\right]\text{dA} \tag{16}$$

The membrane forces N_{ik}^{pre} are those available from the solution of the pre-buckling problem. Note that all the displacement components entering Eq. (16) should be interpreted as variation with respect to the pre-buckling condition.
The quadratic part of the stiffeners' total potential energy is:

$$\delta^2\Pi^i = \frac{1}{2}\int_{\Gamma^i} \begin{Bmatrix} \tilde{\xi}^i \\ \tilde{k}^i \end{Bmatrix}^{\text{T}} C^i \begin{Bmatrix} \tilde{\xi}^i \\ \tilde{k}^i \end{Bmatrix} \text{d}s + \frac{1}{2}\int_{\Gamma^i} P^i \tilde{\eta}_{tt}^i\,\text{d}s \tag{17}$$

where P^i specifies the pre-buckling axial forces carried by the stiffeners.

2.5 Ritz approximation

The approximate solution for the pre-buckling and buckling problem is sought by referring to the Ritz approach. In this framework, the generalized displacement components are expressed using global trial functions. Specifically, the displacements components are expanded as:

$$u_0 = \begin{bmatrix} \phi_{\text{u}}^{\text{T}}(\xi,\eta) & & \\ & \phi_{\text{v}}^{\text{T}}(\xi,\eta) & \\ & & \phi_{\text{w}}^{\text{T}}(\xi,\eta) \end{bmatrix} \begin{Bmatrix} c_{\text{u}} \\ c_{\text{v}} \\ c_{\text{w}} \end{Bmatrix} + \begin{Bmatrix} \overline{\phi}_{\text{u}}(\xi) + \overline{\psi}_{\text{u}}(\eta) \\ \overline{\phi}_{\text{v}}(\xi) + \overline{\psi}_{\text{v}}(\eta) \\ 0 \end{Bmatrix} = \Phi_{\text{u}} a_{\text{u}} + \overline{\Phi}_{\text{u}} \tag{18}$$

where Φ_{u} is a matrix collecting the trial functions – defined here as the product between Legendre polynomials and boundary functions – for the approximation of the three displacement parameters u_0, v_0 and w_0, while the vector a_{u} collects the unknown Ritz amplitudes.

The last vector of Eq. (18), $\overline{\Phi}$, is introduced to consider any prescribed displacement at the four edges, and its entries are:

$$\begin{aligned} \overline{\phi}_{\mathrm{u}} &= \frac{\overline{u}_3 - \overline{u}_1}{2}\xi, \qquad \overline{\psi}_{\mathrm{u}} = \frac{\overline{u}_4 - \overline{u}_2}{2}\eta \\ \overline{\phi}_{\mathrm{v}} &= \frac{\overline{v}_3 - \overline{v}_1}{2}\xi, \qquad \overline{\psi}_{\mathrm{v}} = \frac{\overline{v}_4 - \overline{v}_2}{2}\eta \end{aligned} \tag{19}$$

The expansion for the rotation parameters is operated similarly to Eq. (18). Upon substitution of Eq. (18) into the variational principles (see Eqs. (10) and (15)), and after performing numerical integration, the set of algebraic equations governing the pre-buckling and buckling problem are derived as:

$$Ka = F, \qquad \left(K + \lambda K_{\mathrm{g}}\right) a = 0 \tag{20}$$

where K, K_{g} and M are the assembled stiffness, geometric stiffness and mass matrices of the stiffened panel, while F is the vector of the external loads.

3 Results

The approach is applied to study two test-cases from the literature regarding the mechanical and thermal buckling of panels stiffened by curvilinear stringers. Both concentric and eccentric stiffeners are considered, i.e. $e = 0$ and $e \neq 0$, where e is the stiffener eccentricity, as illustrated in the sketches of Figure 2.

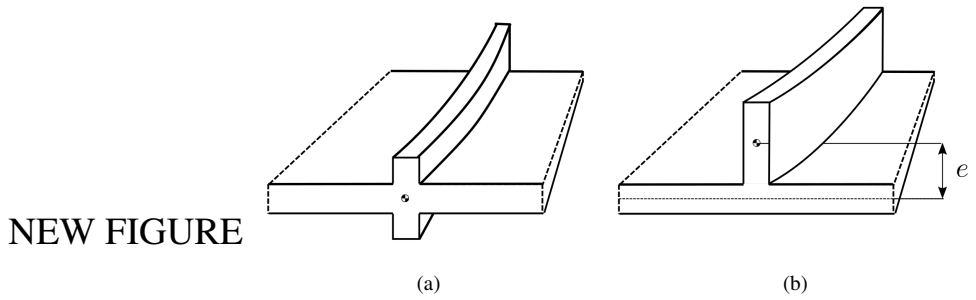

Fig. 2 Stiffener configurations: (a) concentric, (b) eccentric.

An example is then presented to illustrate the potential of the approach in deriving interaction curves for multiple loading conditions.
All the computations are performed using the same number of trial functions for all the displacement components. The corresponding expansion is then indicated as $R \times S$. The number of functions is chosen on the basis of preliminary convergence tests.

3.1 Mechanical buckling curvilinearly stiffened panel

The first benchmark is taken from Ref. [24] and deals with the buckling analysis of a square panel with dimension 300 *mm*. A 16-ply lay-up with sequence $[\pm\theta_1/\pm\theta_2]_{2\mathrm{s}}$ is considered. The panel is stiffened by four stringers of dimensions $2.03 \times 10.16\ mm^2$. All the relevant data are available in Ref. [24] and are not given here for the sake of brevity. The panel is simply-supported at the four edges, and is loaded with a uniform prescribed shortening along the axis x. All the in-plane displacements along the transverse direction are prevented, thus the skin experiences a biaxial pre-stress state.

A preliminary convergence study is illustrated in Table 1 for the pre-buckling and buckling analysis, where the buckling multiplier corresponding to an axial shortening of 0.02 *mm* is reported. A fixed grid of 30 integration points along the two in-plane directions is considered for evaluating the in-plane integrals.

	Concentric ($e = 0$)					Eccentric ($e \neq 0$)				
	R_{buck}					R_{buck}				
R_{pre}	5	10	15	20	25	5	10	15	20	25
3	8.70	7.68	7.50	7.46	7.44	23.78	17.89	17.24	17.06	16.96
5	8.82	7.69	7.49	7.45	7.43	24.82	16.79	16.23	16.06	15.96
10	8.92	7.61	7.40	7.35	7.33	25.57	15.57	14.96	14.79	14.70
15	8.94	7.62	7.41	7.36	7.34	25.65	15.53	14.92	14.75	14.66
20	8.95	7.63	7.42	7.37	7.35	25.67	15.53	14.92	14.75	14.66
25	8.95	7.63	7.42	7.37	7.35	25.68	15.53	14.92	14.75	14.66
FEM ([24]) - NASTRAN ([24])					7.09 - 7.29					14.70 - 14.91

Table 1 Buckling multipliers for simply-supported VS panels with four curvilinear stringers under prescribed axial shortening of 0.02 *mm*. Convergence analysis using $R_{pre} \times R_{pre}$ and $R_{buck} \times R_{buck}$ functions for the pre-buckling and buckling analysis, respectively.

One can assess the convergence of the pre-buckling solution by moving along the rows of the table, while that of the buckling solution can be analyzed moving along the column-wise direction. It is interesting to note the faster convergence achieved for the pre-buckling analysis, where just 15 trial functions are needed. The buckling problem, due to the presence of local modes, is more demanding, and more trial functions are necessary to reach convergence.

The buckling values obtained by means of finite element calculations are also reported in Table 1. Close agreement can be noted between the reference results and those obtained using the present formulation. It should be noted that slight differences are due to different descriptions of the stiffener path, represented here using a minimum least-square technique to fit the Hobby spline representation of Ref. [24].

Pre-buckling stress distributions are reported in Figure 3 for a prescribed axial shortening of 0.02 *mm*. The combined presence of curvilinear stringers and variable fiber orientations is responsible for a relatively complex pattern. To facilitate the understating of the internal load paths, the fiber orientations of plies at θ_1 and θ_2 are reported in Figure 3(a). Looking at the N_{xx} component, load re-distribution towards the edges can be noted as response to fiber steering. The external portion of the panel are indeed the areas where fibers are mostly aligned with the loading direction, thus offering the highest stiffness along the x direction. Local peaks of axial compressions (blue regions) can be seen due to stringers' local stiffening effects.

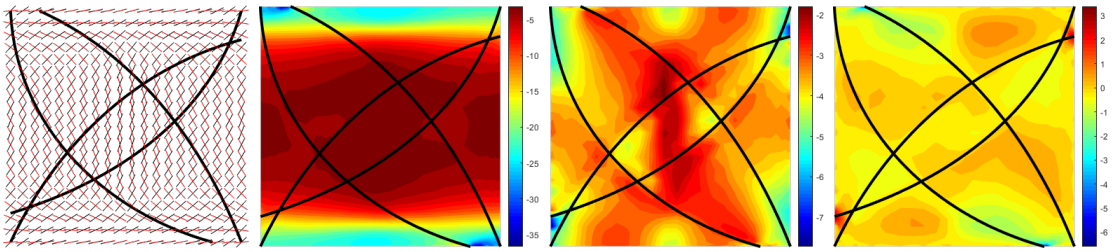

(a) (b) (c) (d)

Fig. 3 Pre-buckling stress resultants for VS panels with four concentric curvilinear stringers under prescribed axial shortening: (a) fiber path (θ_1 black, θ_2 red), (b) N_{xx}, (c) N_{yy}, (d) N_{xy}.

In addition, the comparison of the buckling modes is reported in Figure 4, where the contour refers to the

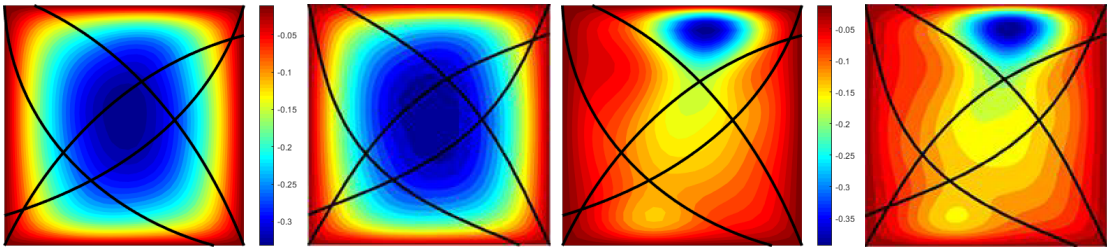

(a) Mode 1, Present (b) Mode 1, Ref. [24] (c) Mode 1, Present (d) Mode 1, Ref. [24]

Fig. 4 Buckling modes for simply-supported VS panels with four curvilinear stringers under prescribed axial shortening: (a)-(b) $e = 0$, (c)-(d) $e \neq 0$.

out-of-plane displacements.
It is observed that, for the concentric case ($e = 0$), the mode displays a global pattern, and all the stiffeners lift from the midsurface. When eccentricity effects are considered, the modal shape is strongly different, and the onset of a local buckle can be noticed in the upper part of the skin. As seen by comparison against reference results, the quality of the predictions is very satisfactory. This is even more true if one considers the small number of degrees of freedom involved in the analysis process, which is equal to 3000, approximately. A similar approach based on finite element calculations, such as the one reported Ref. [24] and where second-order plate element are used, requires a number of dofs which is 6 to 10 times larger.

3.2 Thermal buckling curvilinearly stiffened panel

A second test case deals with the buckling analysis in the presence of a thermal load (Ref. [23]). A composite panel made of carbon/epoxy is considered. The thermal expansions coefficients are $\alpha_1 = -0.9 \cdot 10^{-6} \frac{1}{^\circ C}$ and $\alpha_2 = 27 \cdot 10^{-6} \frac{1}{^\circ C}$, while the remaining elastic properties are available in Ref. [23]. The panel is square with size of 150 mm, and the skin is characterized by a lay-up $[\pm < 69| - 5.705 >]_{2s}$. The two curvilinear stringers have dimensions 1.02×5.08 mm^2, with all the plies oriented at 0 degrees. The panel is subjected to uniform heating, while the in-plane motion along panel edges is prevented, implying that normal and shearing resultants are introduced through edge reactions forces. Simply-supported flexural boundary conditions are considered: out-of-plane displacements are prevented, but all rotations are left free along the boundaries. For clarity, a sketch of the boundary and thermal loading conditions is presented in Figure 5.
The path of the plies at $[+ < 69| - 5.705 >]$ is sketched in Figure 6(a), while the pre-buckling stress distribution is presented in Figures 6(b) to 6(d). It can be observed that the central area of the panel experiences a tensile N_{yy} pre-buckling state, due to the negative thermal expansion coefficient along the fiber direction. On the contrary, the external parts undergo a compressive N_{yy} pre-stress of increasing magnitude as the fibers are progressively aligned with the horizontal direction. Indeed, the positive thermal expansion coefficient along the matrix direction determines a compressive stress as a reaction to the edges' prevented displacement along the y direction.
A summary of the first five critical temperatures is available in Table 2, where the comparison is presented against results from the literature. The results are computed using 20×20 functions, leading to a number of dofs that is 5 to 6 times smaller with respect to the FEM models used in the reference.
Additional results are presented for different sets of flexural boundary conditions, referring to the notation where S stands for simply-supported and C for clamped. Each letter refers to one edge, starting from the one at $x = -a/2$ and rotating in counterclockwise direction.
The quality of the prediction in terms of buckling temperatures can be seen by inspection of Table 2, where a maximum difference of 1.5% is obtained. It is interesting to highlight the strong dependency of the buckling multiplier on the flexural boundary conditions, in particular with respect to the rotational restraint at the first

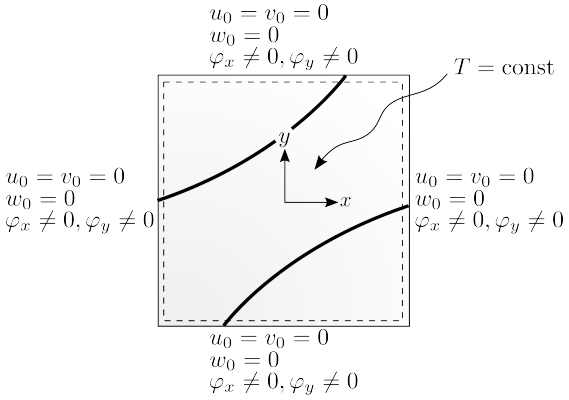

NEW FIGURE

Fig. 5 Boundary conditions for curvilinearly stiffened panel.

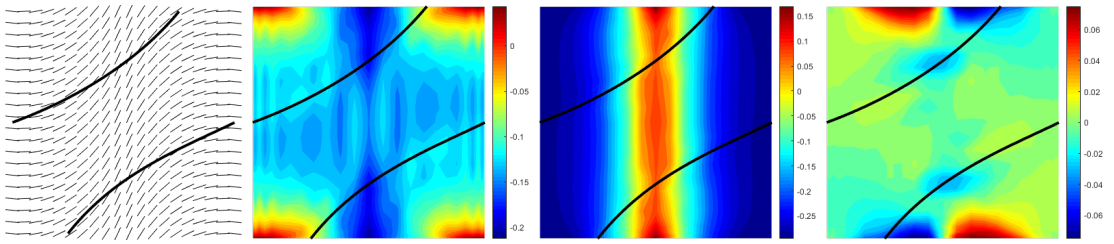

Fig. 6 Pre-buckling stress resultants for VS panels with two concentric curvilinear stringers subjected to unitary thermal heating: (a) fiber path $[+ < 69| - 5.705 >]$, (b) N_{xx}, (c) N_{yy}, (d) N_{xy}.

BC	Mode	Concentric ($e = 0$)			Eccentric ($e \neq 0$)		
		FEM ([23])	NASTRAN ([23])	Ritz 20×20	FEM [23]	NASTRAN ([23])	Ritz 20×20
SSSS	1	77.78	78.00	77.89	101.03	100.92	101.83
	2	117.44	118.07	118.02	122.61	123.27	123.51
	3	138.78	140.06	137.97	150.08	152.25	149.55
	4	143.09	144.65	143.04	151.75	153.83	151.13
	5	149.92	151.97	149.69	160.01	162.38	160.49
SCSC	1	-	-	111.44	-	-	117.42
CSCS	1	-	-	181.17	-	-	195.32
CCCC	1	-	-	202.02	-	-	202.88

Table 2 Critical temperatures ($^\circ C$) for for simply-supported VS panels with two curvilinear stringers under uniform temperature increase.

and third edges.

The comparison with literature results is presented Figure 7, where the first buckled shapes are plotted in terms of out-of-plane deflection contours. As observed, the agreement with the results obtained in Ref. [23] is excellent.

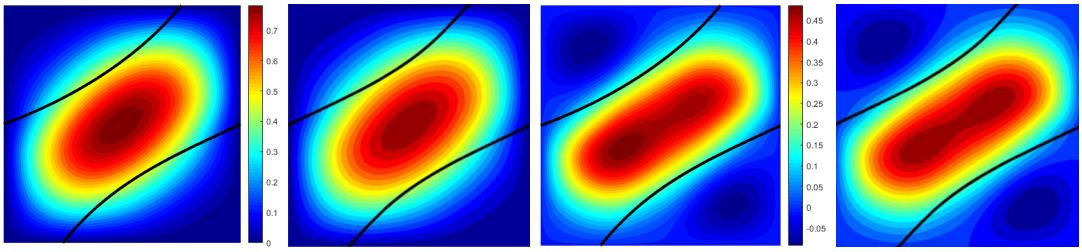

(a) Mode 1, Present (b) Mode 1, Ref. [23] (c) Mode 1, Present (d) Mode 1, Ref. [23]

Fig. 7 Buckling modes for simply-supported VS panels with two curvilinear stringers under uniform temperature increase: (a)-(b) $e = 0$, (c)-(d) $e \neq 0$.

3.3 Thermo-mechanical buckling of curvilinearly stiffened panel

To illustrate the potential of the approach, the thermo-mechanical buckling response is now assessed for the same configuration discussed in the previous example. The panel, which is stiffened by means of two concentric stiffeners, is subjected to a combination of mechanical loads, introduced by means of a prescribed uniform displacement applied at the two parallel edges at $x = \text{const}$, and a uniform temperature variation. Two different sets of in-plane boundary conditions are considered and denoted hereinafter as B1 and B2. In the first case (B1 condition) the transverse contraction/expansion is prevented by enforcing the displacement component v to vanish along the two edges at $y = \text{const}$. This condition is inherently biaxial, as thermally-induced resultants N_{yy} are promoted by retaining the transverse displacements. In the second case (B2 condition), no essential boundary conditions are imposed at the edges at $y = \text{const}$, so the transverse resultant N_{yy} develops internally due to stiffness variability, but is not introduced at the edges in the form of reaction forces. Regarding the flexural behaviour, two sets of conditions are considered, and are denoted next as SSSS and CSCS. Note, the letter S specifies here prevented out-of-plane deflection and free rotations ϕ_x, ϕ_y, whilst C defines prevented out-of-plane deflections and rotations. Nothing is implied with respect to the in-plane displacement degrees of freedom.

The results are summarized in the interaction curves of Figure 8, where positive values of ΔU denote axial shortening, whilst heating and cooling are associated with positive and negative values of the temperature variation T, respectively. Each point of the curves corresponds to one single buckling analysis. Hence, several repeated runs are needed to obtain these plots, further providing evidence of the advantages offered by a model characterized by relatively few degrees of freedom.

The plots summarize the first buckling modes obtained for different ratios between prescribed temperature and axial displacement, furnishing an overview of the modal changes experienced by the panel when the loading conditions are modified.

Referring to Figure 8, it is noted that pre-buckling stress resultants do not depend on the flexural boundary conditions. Indeed, the symmetry of the skin stacking sequence and the presence of concentric stiffeners lead to uncoupled membrane and bending behaviour. Therefore any difference between SSSS and CSCS configurations is fully due to the bending-related response of the panel. The effect of adding constraints, which is well known in classical buckling theory, is noticeable, inasmuch preventing the loaded edges from rotation has the effect of strongly improving the buckling loads. For positive temperatures, i.e. heating, the skin experiences a compressive resultant N_{xx} along with a pattern of N_{yy} where the central region is subjected to traction and the outer regions to compression – one can refer to Figure 6 for the pre-buckling contour plot relative to a set of boundary conditions similar to the case B1. In case of cooling, the patterns are reversed, with tensile N_{xx} (in average) over the domain and transverse resultant N_{yy} characterized by a compressively loaded inner region. This help explaining the buckled patterns available in the plots of Figure 8. The negative side of the y-axis (cooling) corresponds to pre-buckling compressive forces affecting the central part of the structure, where the buckle tends to localize. For positive temperature changes, the central part of the structure is stabilized through tensile transverse stresses, whilst the outer parts are subjected to biaxial compression. Buckling deflections are

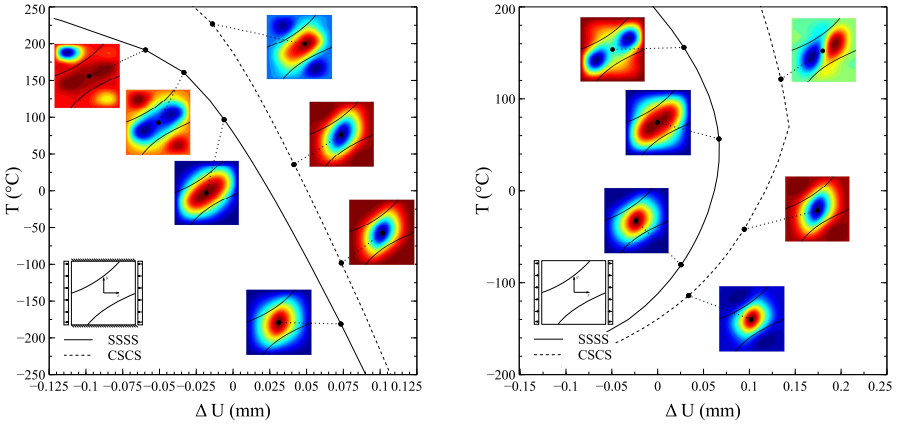

Fig. 8 Interaction curve for VS panels with two concentric curvilinear stringers and subjected to combined thermo-mechanical loads. In-plane conditions: (a) B1, (b) B2.

thus promoted in the outer parts the structure, leading to larger halfwave lengths and, eventually, to buckling localization. It is interesting to notice that the slope of the interaction plots tends to remain constant as the buckled shape is preserved, whilst changes of slope are accompanied by modal changes.

4 Conclusions

The work discussed a fast numerical approach for the pre-buckling and buckling analysis of composite stiffened panels, where the skin can be characterized by non-uniform stiffness properties and the stiffeners can run along curvilinear paths described by Bézier splines. The comparison with reference finite element calculations demonstrates the accuracy of the approach proposed. Main advantages are the reduced number of degrees of freedom involved in the computations along with the ease in generating the models. These aspects render the formulation particularly suitable for those cases where several analysis need to be run, such as in the early steps of the design phase. Furthermore, the ease in generating and analyzing relatively complex configurations allows to perform parametric studies and preliminary optimizations, which can be useful for gathering understanding into the mechanical response of curvilinearly stiffened panels. While the combined effects of VS skin and curvilinear stringer can be exploited for achieving improved buckling response, future work should be directed towards the introduction of blending requirements between the skin and stiffeners.

Conflict of interest

On behalf of all authors, the corresponding author states that there is no conflict of interest.

References

1. Z. Wu, P.M. Weaver, G. Raju, and B.C. Kim. Buckling analysis and optimisation of variable angle tow composite plates. *Thin-Walled Structures*, 60:163–172, 2012.
2. Z. Wu, G. Raju, and P.M. Weaver. Postbuckling analysis of variable angle tow composite plates. *International Journal of Solids and Structures*, 50(10):1770–1780, 2013.
3. R. Vescovini and L. Dozio. A variable-kinematic model for variable stiffness plates: Vibration and buckling analysis. *Composite Structures*, 142:15–26, 2016.
4. R. Vescovini, E. Spigarolo, E. Jansen, and L. Dozio. Efficient post-buckling analysis of variable-stiffness plates using a perturbation approach. *Thin-Walled Structures*, 143:106211, 2019.
5. S.F. Pitton, S. Ricci, and C. Bisagni. Buckling optimization of variable stiffness cylindrical shells through artificial intelligence techniques. *Composite Structures*, 230, 2019.
6. R. Vescovini and L. Dozio. Thermal buckling behaviour of thin and thick variable-stiffness panels. *Journal of Composites Science*, 2(4):1–23, 2018.
7. A. Viglietti, E. Zappino, and E. Carrera. Analysis of variable angle tow composites structures using variable kinematic models. *Composites Part B: Engineering*, 171:272–283, 2019.
8. R.K. Kapania, J. Li, and H. Kapoor. Optimal design of unitized panels with curvilinear stiffeners. In *AIAA* 5^{th} *Aviation, Technology, Integration, and Operations Conference (ATIO)*, AIAA 2005-7482, Arlington, VA, 26–28 September 2005.
9. P. Joshi, S. Mulani, R.K. Kapania, and Y. Shin. Optimal design of unitized structures with curvilinear stiffeners using response surface methodology. In 49^{th} *AIAA/ASME/ASCE/AHS Structures, Structural Dynamics and Material Conference*, AIAA 2008-2304, Schaumburg, IL, April 7–10 2008.
10. S.P. Gurav and R.K. Kapania. Development of framework for the design optimization of unitized structures. In 50^{th} *AIAA/ASME/SAE Structures, Structural Dynamics and Materials Conference*, AIAA 2009-2186, Palm Springs, CA, May 4–7 2009.
11. P. Shi, R.K. Kapania, and C.Y. Dong. Vibration and buckling analysis of curvilinearly stiffened plates using finite element method. *AIAA Journal*, 53(5):1319–1335, 2015.
12. W. Zhao and R.K. Kapania. Buckling analysis of unitized curvilinearly stiffened composite panels. *Composite Structures*, 135:365–382, 2016.
13. W. Zhao and R.K. Kapania. Vibration analysis of curvilinearly stiffened composite panel subjected to in-plane loads. *AIAA Journal*, 55(3):981–997, 2017.
14. A.Y. Tamijani and R.K. Kapania. Vibration of plate with curvilinear stiffeners using mesh-free method. *AIAA Journal*, 48(8):1569–1581, 2010.
15. A.Y. Tamijani and R.K. Kapania. Buckling and static analysis of curvilinearly stiffened plates using mesh-free method. *AIAA Journal*, 48(12):2739–2751, 2010.
16. A.Y. Tamijani and T. McQuigg R.K. Kapania. Free vibration analysis of curvilinear-stiffened plates and experimental validation. *Journal of Aircraft*, 47(1):192–200, 2010.
17. A.Y. Tamijani and R.K. Kapania. Chebyshev-Ritz approach to buckling and vibration of curvilinearly stiffened plate. *AIAA Journal*, 50(5):1007–1018, 2010.
18. R. Fernandes and A.Y. Tamijani. Flutter analysis of laminated curvilinear-stiffened plates. *AIAA Journal*, 55(3):998–1011, 2017.
19. R. Vescovini, V. Oliveri, D. Pizzi, L. Dozio, and P.M. Weaver. A semi-analytical approach for the analysis of variable-stiffness panels with curvilinear stiffeners. *International Journal of Solids and Structures*, 2019.
20. K. Yoshida, S. Sadamoto, Y. Setoyama, S. Tanaka, T.Q. Bui, C. Murakami, and D. Yanagihara. Meshfree flat-shell formulation for evaluating linear buckling loads and mode shapes of structural plates. *Journal of Marine Science and Technology*, 22(3):501–512, 2017.
21. M. Ozdemir, S. Sadamoto, S. Tanaka, S. Okazawa, T.T. Yu, and T.Q. Bui. Application of 6-DOFs meshfree modeling to linear buckling analysis of stiffened plates with curvilinear surfaces. *Acta Mechanica*, 229(12):4995–5012, 2018.
22. K. Singh and R.K. Kapania. Optimal design of tow-steered composite laminates with curvilinear stiffeners. In *2018 AIAA/ASCE/AHS/ASC Structures, Structural Dynamics, and Materials Conference*, AIAA 2018-2243, Kissimmee, FL, 8–12 January 2018.
23. W. Zhao, K. Singh, and R.K. Kapania. Thermal buckling analysis and optimization of curvilinearly stiffened plates with variable angle tow laminates. *Journal of Spacecraft and Rockets*, pages 1–16, 2019.
24. W. Zhao and R.K. Kapania. Prestressed vibration of stiffened variable-angle tow laminated plates. *AIAA Journal*, pages 1–19, 2019.
25. C. Bisagni and R. Vescovini. Analytical formulation for local buckling and post-buckling analysis of stiffened laminated panels. *Thin-Walled Structures*, 47(3):318–334, 2009.
26. C. Bisagni and R. Vescovini. Fast tool for buckling analysis and optimization of stiffened panels. *Journal of Aircraft*, 46(6):2041–2053, 2009.
27. R. Vescovini and C. Bisagni. Buckling analysis and optimization of stiffened composite flat and curved panels. *AIAA Journal*, 50(4):904–915, 2012.
28. B.H. Coburn, Z. Wu, and P.M. Weaver. Buckling analysis of stiffened variable angle tow panels. *Composite Structures*, 111:259–270, 2014.
29. V. Oliveri, A. Milazzo, and P.M. Weaver. Thermo-mechanical post-buckling analysis of variable angle tow composite plate assemblies. *Composite Structures*, 183:620–635, 2018.

30. I. Benedetti, V. Gulizzi, and A. Milazzo. X-Ritz solution for nonlinear free vibrations of plates with embedded cracks. *Aerotecnica Missili & Spazio*, 98(1):75–83, 2019.
31. J.N. Reddy. *Energy Principles and Variational Methods in Applied Mechanics*. John Wiley and Sons, New York, USA, 1984.
32. L. Martini and R. Vitaliani. On the polynomial convergent formulation of a C^0 isoparametric skew beam element. *Computers & Structures*, 29(3):437–449, 1988.
33. J.C. Massa and E.J. Barbero. A strength of materials formulation for thin walled composite beams with torsion. *Journal of Composite Materials*, 32(17):1560–1594, 1998.